DMD Fast Forward. Published on September 19, 2006 as doi:10.1124/dmd.106.012286

Metabolic Aromatization of N-Alkyl-1,2,3,4-Tetrahydroquinoline Substructures to Quinolinium by Human Liver Microsomes and Horseradish Peroxidase

Chungang Gu, Roxane Collins, Daniel D. Holsworth, Gregory S. Walker, and Richard L. Voorman

Pfizer Global Research and Development, Pharmacokinetics Dynamics & Metabolism (C.G., R.C., G.S.W., R.L.V.); Department of Chemistry (D.D.H.), Ann Arbor, Michigan

DMD Fast Forward. Published on September 19, 2006 as DOI: 10.1124/dmd.106.012286
This article has not been copyedited and formatted. The final version may differ from this version.

Running Title: **Quinolinium Metabolites**

Corresponding author: Chungang Gu, Ph.D.

Pfizer Global Research and Development

2800 Plymouth Rd

Ann Arbor, MI 48105

Tel: 734-622-5368

Email: chungang.gu@pfizer.com

Number of Text Pages	*33*	
Number of Tables	*2*	
Number of Schemes	*3*	
Number of Figures	*7*	
Number of References	*37*	*(Maximum limit 40)*
Number of Words in Abstract	*241*	*(Maximum limit 250)*
Number of Words in Introduction	*555*	*(Maximum limit 750)*
Number of Words in Discussion	*1477*	*(Maximum limit 1500)*

ABBREVIATIONS:

CYP or P450, cytochrome P450; HLM, human liver microsomes; HRP, horseradish peroxidase; IE, ionization energy; LC, liquid chromatography; MAO, monoamine oxidase; MS, mass spectrometry; MPP^+, 1-methyl-4-phenylpyridinium; MPTP, 1-methyl-4-phenyl-1,2,3,6-tetrahydropyridine; NMR, nuclear magnetic resonance; TOCSY, total correlated spectroscopy (a two-dimensional NMR); SET, single-electron transfer.

ABSTRACT

Metabolic aromatization of xenobiotics is an unusual reaction with some documented examples. For instance, the oxidation of 1-methyl-4-phenyl-1,2,3,6-tetrahydropyridine (MPTP) to the neurotoxic pyridinium ion metabolite 1-methyl-4-phenylpyridinium (MPP^+) by monoamine oxidase (MAO) B in the brain has been of interest to a number of investigators. It has also been reported that, while the aromatization of N-methyl-tetrahydroisoquinoline occurs with MAO B, the metabolism does not proceed for its isomer, N-methyl-tetrahydroquinoline, by the same enzyme. The aromatization of an N-alkyl-tetrahydroquinoline substructure was identified during *in vitro* metabolite profiling of compound **A** – designed as a potent renin inhibitor for the treatment of hypertension. The N-alkylquinolinium metabolite of compound **A** was identified by LC-MS/MS of human liver microsomal incubates and proton NMR of the isolated metabolite. Further *in vitro* metabolism studies with a commercially available chemical (compound **B)**, containing the same substructure, also generated an N-alkylquinolinium metabolite. *In vitro* cytochrome P450 (CYP) reaction phenotyping of compound **A** revealed that the metabolism was catalyzed exclusively by CYP3A4. Although compound **B** was a substrate for several CYP isoforms, its quinolinium metabolite was also generated predominantly by CYP3A4. Neither compound **A** nor **B** was a substrate of MAOs. The quinolinium metabolites were readily produced by horseradish peroxidase, suggesting that aromatization of the N-alkyltetrahydroquinoline could occur via a mechanism involving single electron transfer from nitrogen. Although dihydro intermediates from the tetrahydroquinoline substrates were not observed in the formation of quinolinium metabolites, cyanide trapping results indicated the occurrence of iminium intermediates.

Compound **A** (Scheme 1) was a lead compound consisting of a novel non-peptidic ketopiperazine-based scaffold, that was designed as a potent renin inhibitor for the treatment of hypertension (Holsworth et al., 2005 & 2006). The renin-angiotensin system (RAS) plays a key role in blood pressure regulation. Pharmacological blockade of the RAS cascade is usually achieved with angiotensin coverting enzyme (ACE) inhibitors or angiotensin receptor blockers (ARBs). Renin inhibition has been sought for decades, as it would inhibit the initial and rate-limiting step of the RAS, and hence might offer a therapeutic profile distinct from ACE inhibitors and ARBs. Recent progress shows new potential for the treatment of hypertension by renin inhibition (Fisher and Hollenberg, 2005; Wood et al., 2005).

During *in vitro* metabolite profile studies on compound **A**, in support of lead optimization, an unusual metabolite was observed. It appeared to be derived from aromatization of the N-alkyltetrahydroquinoline ring, yielding an N-alkylquinolinium ion as a major metabolite in human liver microsomes. Similar metabolic oxidation of 1-methyl-4-phenyl-1,2,3,6-tetrahydropyridine (MPTP) to the neurotoxic pyridinium metabolite, 1-methyl-4-phenylpyridinium (MPP^+), by monoamine oxidase B (MAO-B) in the brain (Scheme 2), as well as the aromatization of a variety of MPTP's derivatives, have been previously described (Castagnoli et al., 2002; Di Monte et al., 1996; Gerlach et

at 1991; Maret et al., 1990). Recently, a study of electrochemistry-electrospray mass spectrometry on the electrochemical oxidation of N-alkyl-4-phenyl-1,2,3,6-tetrahydropyridinyl derivatives and the chemical fate of the resulting aminyl radical cations has presented a unique perspective in understanding the metabolic oxidation mechanism for the tetrahydropyridines (Jurva et al., 2005). Also illustrated in Scheme 2 is the formation of N-methyl-isoquinolinium from N-methyl-tetrahydroisoquinoline by MAO B (Booth et al., 1989; Naoi et al., 1989). Two more examples of the similar aromatization have been reported in this journal; one involving an N-alkyl-5-tetrazolyl-1,2,3,6-tetrahydropyridine substructure (Christensen et al., 1999) and another with an N-alkyl-4,5,6,7-tetrahydro-thieno[3,2-*c*]pyridine substructure (Dalvie and O'Connell, 2004). The substrates in these reports all have remarkably similar substructures in that the cyclic tertiary nitrogen is distal to a carbon-carbon double bond or an aromatic ring by a methylene unit. Fascinatingly, when the nitrogen atom was "moved" from this type of distal position (as in N-methyl-tetrahydroisoquinoline; Scheme 2) to the direct attachment on an aromatic ring (as in N-methyl-tertrahydroquinoline; Scheme 2), the latter isomer (N-methyl-tetrahydroquinoline) was no longer a substrate of the same enzyme (MAO-B) that metabolized the former compound (N-methyl-tetrahydroisoquinoline) (Booth et al., 1989). Shaffer et al. have reported the horseradish peroxidase (HRP) mediated conversion of N-cyclopropyl-N-methylaniline to N-methyl-quinolinium ion (Scheme 2), via a proposed intermediate of 1-methyl-3,4-dihydroquinolinium (Shaffer et al., 2001). In contrast, cytochrome P450 catalyzed oxidation of N-cyclopropyl-N-methylaniline did not generate the quinolinium metabolite, rather the P450s yielded common phase-I metabolites (e.g., demethyl, decyclopropyl, and

p-hydroxy metabolites) in liver microsomes from phenobarbital pretreated rats (Shaffer et al., 2002).

In addition to the quinolinium metabolite of compound **A**, we have also investigated if a similar N-alkylquinolinium metabolite could be generated in liver microsomes from a commercially available compound, 2-(3,4-dihydro-1(2H)-quinolinyl)-N-(4-ethoxyphenyl)acetamide (Scheme 1; referred to as compound **B** hereafter), that also contains an N-alkyltetrahydroquinoline substructure. Besides metabolite structural identification, enzyme phenotyping was also done on both compounds (**A** and **B**) using a panel of cDNA-expressed cytochrome P450 (CYP) isoforms, MAOs, and HRP. Furthermore, cyanide trapping experiments were performed to search for postulated iminium intermediates in the formation of the quinolinium metabolites.

MATERIALS AND METHODS

Materials. Compound **A** was synthesized as described by Holsworth et al. (2005). Compound **B**, i.e. 2-(3,4-dihydro-1(2H)-quinolinyl)-N-(4-ethoxyphenyl)acetamide, was purchased from Sigma-Aldrich (catalog R713775; CAS 303091-40-9). Human liver microsomes were purchased from In Vitro Technologies (catalog HL-Mix-14). The following P450 BACULOSOMES® were purchased from Panvera and assayed for reaction phenotyping – CYP1A2 (catalog P2792), CYP2B6 (catalog P3028), CYP2C9 (catalog P2378), CYP2C19 (catalog P2570), CYP2D6 (catalog R1627), CYP2E1 (catalog

P2223) and CYP3A4 (catalog P2377). The BACULOSOMES® are microsomes prepared from insect cells infected with a recombinant baculovirus containing a human P450 isozyme and a rabbit NADPH-P450 reductase. In addition, the following P450 Supersomes™ were purchased through Gentest and also assayed for reaction phenotyping – CYP2A6 (catalog 456254) and CYP2C8 (catalog 456252). The Supersomes™ are microsomes prepared from insect cells infected with a recombinant baculovirus containing a human P450 isozyme, NADPH-P450 reductase and cytochrome b_5. Horseradish peroxidase (catalog P2088), catalase from bovine liver (catalog C40), monoamine oxidase A (catalog M7316) and monoamine oxidase B (catalog M7441) were purchased from Sigma-Aldrich.

Human Liver Microsomal Incubations. Each 3 mL human liver microsomal (HLM) incubation was carried out in 50 mM potassium phosphate buffer pH 7.4. Incubation mixtures contained NADPH at 1 mM final concentration, 1 mg/mL final protein concentration and 50 μM final substrate concentration (compound **A** or **B**). Negative controls were set up in the absence of NADPH. All components except substrate were added to reaction mixtures on ice. The mixtures were pre-incubated for 3 min at 37°C in a shaking water bath, and then substrate (5 mM stock solution in methanol) was added to initiate reactions. Reactions were terminated at 90 min by quenching with ice-cold acetonitrile at a 1:1 ratio.

To isolate metabolites using preparative LC, large-scale (100 mL) HLM incubations were carried out (10 Erlenmeyer flasks containing 10 mL each) using the same concentrations and incubation time as described above. Quenched reaction mixtures were concentrated

down to ~15-20 mL under vacuum at room temperature using a SpeedVac (Thermo Electron Corp).

Cyanide (CN^-) trapping of iminium intermediates. Each 1 mL incubation was carried out in 50 mM potassium phosphate buffer pH 7.4. Incubation mixtures contained 1 mg/mL final protein concentration of pooled human liver microsomes (HLM), 1 mM NADPH, 50 μM substrate (compound **A** or **B**), and 1 mM potassium cyanide (KCN). Negative controls were set up in the absence of human liver microsomes and NADPH. The mixtures were incubated at 37°C in a shaking water bath for 60 min and then the reactions were terminated by quenching with ice-cold acetonitrile at a 1:1 ratio.

Reaction Phenotyping with cDNA-Expressed Cytochrome P450 Enzymes. P450 BACULOSOMES® and Supersomes™ incubations were carried out in 50 mM potassium phosphate buffer pH 7.4. Incubation mixtures contained NADPH at 1 mM final concentration, 0.5 mg/mL final total BACULOSOMES® or Supersomes™ protein concentration and 50 μM final concentration of substrate. The incubation volume was 1 mL. All components except drug were added to vials on ice, then the vials were pre-incubated for 3 min at 37°C in a shaking water bath for 3 min, and then substrate was added to vials to initiate reactions. Reactions were terminated at 90 min by quenching with ice-cold acetonitrile at a 1:1 ratio.

Horseradish Peroxidase Incubations. Horseradish peroxidase (HRP) incubations were carried out in 50 mM potassium phosphate buffer pH 7.4. Incubation mixtures contained

HRP at 30 units/mL final concentration, 500 μM final hydrogen peroxide (H_2O_2) concentration and 50 μM final substrate concentration (compound **A** or **B**). The incubation volume was 1 mL. Negative controls were set up in the absence of either HRP or H_2O_2. All components except substrate were added to reaction mixtures on ice. Reactions were pre-incubated for 3 min at 37°C in a shaking water bath, and then substrate was added to initiate reactions. Reactions were terminated at 45 min with the addition of catalase at 300 units/mL final concentration. After an additional 3 min at 37°C in a shaking water bath, reactions were quenched with ice-cold acetonitrile at a 1:1 ratio.

MAO A and MAO B Incubations. Each 1 mL incubation was carried out in 50 mM potassium phosphate buffer pH 7.4. Incubation mixtures contained 50 μM final substrate concentration (compound **A** or **B**) and MAO A or MAO B at 0.36 mg/mL or 0.83 mg/mL final concentration, respectively. Positive controls for both MAO A and MAO B were set up with kynuramine dihydrobromide at a final substrate concentration of 50 μM. Reactions were pre-incubated for 3 min at 37°C in a shaking water bath, and then substrate was added to initiate reactions. Reactions were terminated at 45 min by quenching with ice-cold acetonitrile at a 1:1 ratio.

LC-MS and Preparative LC. All quenched reaction mixtures (HLM, CYPs, MAOs, HRP, or CN^- trapping) were vortexed and centrifuged at 14,000 rpm in an Eppendorf 5804R centrifuge for 20 min at 4°C to pellet proteins. 20 μL aliquots of the supernatants were injected for LC-MS or MS/MS analysis, as summarized in Table 1.

A 5 mL aliquot of the concentrated supernatant of the large-scale HLM incubation was injected into a 21.20 mm ID preparative column. The metabolites were separated as described in Table 1 and collected by the fraction collector of the preparative LC system. Fractions of the same metabolite from multiple injections were combined and the solvent was evaporated till dry under vacuum at room temperature using a SpeedVac.

^{1}H NMR: All samples were dissolved in 0.1 ml of methanol-d_4 "100%" (Cambridge Isotope Laboratories, Andover, MA). ^{1}H and TOCSY spectra were referenced using residual methanol-d_4 (δ=3.31 ppm relative to TMS, δ=0.00).

All NMR spectra were recorded on a Bruker Avance 600 MHz (Bruker BioSpin Corporation, Billerica, MA) controlled by XWIN-NMR V3.5 and equipped with a 2.5 mm BBI probe. One-dimensional spectra were recorded using a sweep width of 8000 Hz and a total recycle time of 5 s. The resulting time-averaged free induction decays were transformed with an exponential line broadening of 0.3 Hz to enhance signal to noise.

The two-dimensional TOCSY data were recorded using the standard pulse sequence provided by Bruker. A 1K x 128 data matrix was acquired using 32 scans and 16 dummy scans with a spectral width of 6600 Hz. A mixing time of 80 ms was used. The data was zero-filled to a size of 1K x 1K. A relaxation delay of 2 s was used between transients.

RESULTS

The pooled human liver microsomal incubation of compound **A** generated several metabolites (Fig 1), including common phase-I metabolites undergoing *O*-dealkylation (M_A4 & M_A6) or phenyl hydroxylation (M_A5). An unusual metabolite (M_A3), with a molecular ion m/z value at 4-Dalton less than parent drug, was observed as the most abundant metabolite in both the mass spectrometric total ion chromatogram (TIC) and the UV chromatogram (Fig. 1). In addition, sequential metabolites undergoing the unusual metabolic pathway (4-Dalton loss) and a common phase-I metabolic pathway (either *O*-dealkylation or phenyl hydroxylation) were also detected (M_A1 or M_A2, respectively; Fig 1).

The LC-MS/MS product ion spectra of M_A3 vs. parent drug (Fig. 2; panels b vs. a) indicated that the 4-Dalton loss occurred within the 1,7-disubstituted-1,2,3,4-tetrahydroquinoline substructure of compound **A**. Collective evidence was gathered from the unchanged fragments at m/z 383 (panel a & b), a 4-Dalton shift to lower mass from the original fragments m/z 235 & 532 of the parent to m/z 231 & 528 of M_A3 (panel b vs. a), and a new fragment ion of M_A3 at m/z 146 (panel b). Desaturation of the tetrahydroquinoline ring by three hydrogen atoms and the concurrent formation of quinolinium, which eliminates the need for an ionizing proton, would yield a 4-Dalton loss (see chemical structures in Fig. 2). High confidence in the structural elucidation of the quinolinium metabolite by MS/MS (Fig 2b) was built upon the reliable MS/MS spectral interpretation of the parent drug (Fig 2a), which was verified beforehand with a

DMD Fast Forward. Published on September 19, 2006 as DOI: 10.1124/dmd.106.012286
This article has not been copyedited and formatted. The final version may differ from this version.

common metabolite (M_A5, formed via phenyl hydroxylation) exhibiting fragmentation patterns similar to parent drug, i.e., the predicted fragments of the metabolite (M_A5) all appeared in its MS/MS spectrum at expected m/z ratios (spectrum not shown). The diagnostic MS/MS spectra in Figure 2 were acquired by a triple quadrupole instrument. Whereas, initial MS/MS experiments in an ion-trap mass spectrometer induced only a selective cleavage resulting in m/z 532 and 528 fragments for parent drug and M_A3, respectively. Subsequent MS^3 experiments of either m/z 532 or 528 fragments produced only a single further fragment — formed by a neutral loss of 108. In short, ion trap fragmentation was insufficient for the structural identification.

The NMR characterization of the isolated metabolite, M_A3, confirmed the formation of the quinolinium structure. The aromatic regions of the one-dimensional ^1H NMR spectra of the metabolite and the parent drug are provided in Fig 3 (panel a vs. b). Fourteen aromatic protons were observed in the spectrum of the metabolite, three greater than observed in the spectrum of the parent drug. The three new aromatic protons occur between 7.8 and 9.1 ppm (protons a, b, and c; Fig 3a). Additionally, the aromatic protons of the quinolinium that correlate with the aromatic protons of the tetrahydroquinoline are noticeably shifted toward the lower field (protons d, e, and f; Fig 3a vs. 3b). The ^1H-^1H coupling correlations observed in the TOCSY data (Fig 3c) provide evidence for the chemical shifts assignments. The TOCSY data clearly reveals two independent spin systems, each composed of three protons; 7.86, 9.04, and 9.11 ppm (a, b, and c) and 7.64, 7.94, and 8.29 ppm (e, f, and d, respectively). The coupling patterns and coupling constants also support these spectral assignments. The observed chemical shifts of the

quinolinium protons (especially a & c) of the metabolite are in agreement with what was reported 30 years ago for quinolinium ions generated by dissolving quinoline and seven individual monomethyl derivatives in DCl-D_2O (Barbieri et al., 1975). Both the metabolite and the parent drug analyzed in the NMR experiments were isolated with formic acid present in the mobile phase of the preparative LC. As a result, the aldehyde proton of formic acid (and formate) was observed in the NMR spectra at δ ~8.6 ppm with two ^{13}C satellite peaks (Fig 3).

The human liver microsomal incubation of the commercially available compound **B,** consisting of an N-substituted-tetrahydroquinoline substructure, also produced a metabolite that was characterized by a 4-Dalton loss from parent drug (M_B1, Fig 4), albeit it was a relatively minor metabolite as indicated by the UV signal response (UV chromatogram not shown). Dramatic changes in the MS/MS fragmentation patterns from parent compound to the metabolite can be readily explained by the formation of a quinolinium structure (Fig 5b vs. a). Supporting evidence also came from active hydrogen/deuterium (H/D) exchange accomplished in an LC-MS experiment using D_2O with deuterated acetic acid as the aqueous mobile phase. Compound **A** has one active hydrogen atom located at the acyl aniline nitrogen. The "molecular mass" of M_B1 increased by only one Dalton after the H/D exchange (Table 2, Row of M_B1), which is consistent with M_B1 not requiring an ionizing H/D in electrospray ionization. Otherwise a two-Dalton increase, as noticed in parent drug (Table 2), would have been observed.

In the presence of 1 mM KCN added to a human liver microsomal incubation with compound **A** or **B**, a cyano adduct was observed for each compound. For example, the

ion chromatogram of the reaction mixture for compound **B (**Fig 4b) indicates the formation of a cyano adduct (m/z 336) of compound **B** (m/z 311), coupled with the corresponding diminished abundances of metabolites M_B1 (the N-alkylquinolinium) and M_B8. LC-MS/MS spectra of the cyano adduct of compound **A** (not shown) or **B** (Fig 5c) pinpointed the tetrahydroquinoline moiety as the location of cyano group for both adducts. More specifically, the loss of a HCN neutral molecule in MS/MS fragmentation of both cyano adducts suggested that the cyano group was on the tetrahydro saturated portion of the substructure. As supporting evidence to the spectral interpretation in Fig 5c, further fragmentation of fragment ion m/z 309, i.e., the fragment by the loss of a neutral HCN from the cyano-adduct of compound **B**, produced fragment ions m/z 144, 150 and 281 (spectrum not shown). It was not determined whether the loss of a C_2H_4 or a CO (e.g., via rearrangement), both having a nominal mass of 28 Dalton, contributed to the formation of fragment m/z 150 (Fig 5b & c). The cyano group is drawn on the carbon adjacent to the nitrogen in the chemical structure shown in Fig 5c, as rationalized by the cyanide addition reaction to iminium, although its exact location on the ring can not be determined by MS/MS spectra.

Cytochrome P450 (CYP) reaction phenotyping was performed using a panel of cDNA-expressed enzymes – 1A2, 2A6, 2B6, 2C8, 2C9, 2C19, 2D6, 2E1, and 3A4. Among the CYPs investigated, the metabolism of compound **A** was catalyzed exclusively by CYP3A4. On the other hand, compound **B** was the substrate for a number of CYP isoforms. From the disappearance of parent drug (illustrated in Fig 6), it is evident that multiple CYPs, such as 2C19, 2D6 and 3A4, can extensively metabolize compound **B**.

The reaction phenotying results of compound **B** are also presented in the format of metabolite formation (Fig 7). Chemical structures of the metabolites drawn in Fig 7 are based on interpretation of LC-MS/MS product ion spectra (not shown, except M_B1 in Fig 5), as well as active H/D exchange results (Table 2). For example, a hydroxylation would result in the increase of an exchangeable hydrogen atom (e.g., M2 & 6, Table 2). The quinolinium metabolite (M_B1) of compound **B** was generated predominantly by CYP3A4, with a minor contribution from CYP2C19 (Fig 7). Whereas, common phase-I metabolites of compound **B** were produced by different CYPs, e.g., *O*-deethylation by 2D6 and 2C19 (M4, Fig 7) and hydroxylation at two different sites by a number of CYPs (M2 & 6, Fig 7). The regioselectivity of CYP2D6 on metabolizing compound **B** appeared evident in that CYP2D6 produced only one metabolite, *O*-deethylation M_B4 (Fig 7). It has been known in the literature that drugs metabolized by CYP2D6 contain a basic nitrogen atom and a flat hydrophobic region coplanar to the oxidation site which is approximately either 5 Å (e.g., debrisoquine) or 7 Å (e.g., dextromethorphan; 7~8 Å to be more precise) away from the basic nitrogen atom (de Groot, 1996 & 1997). It is uncertain at present if the tetrahydroquinoline nitrogen atom is indeed the docking site of compound **B –** to fit into a 7 Å model within CYP2D6.

Incubations of either compound **A** or **B** with human recombinant MAO A or MAO B did not generate any metabolites. The incubation experiments with MAO enzymes were validated by a positive control, kynuramine — a known substrate for both MAO A and MAO B. LC-UV-MS indicated that both enzymes were active in generating kynuramine's metabolite, 4-hydroxyquinoline, at high yields.

Quinolinium metabolites of both compound **A** and **B** were generated in significant amounts from the horseradish peroxidase (HRP) incubations. The quinolinium metabolite M_A3 was virtually the only metabolite observed, with less than 1% parent drug remaining after the HRP incubation (chromatogram not shown). The HRP incubation results for compound **B** are displayed with the CYP reaction phenotyping results, in Fig 6 and Fig 7. Among the eight metabolites of compound **B** observed in human liver microsomes (Fig 7), only the quinolinium metabolite (M_B1) and another metabolite (M_B7) were detected in the HRP incubation mixture. The sum of metabolites (M_B1 and M_B7) in HRP accounted for only ~21% of compound **B** derived LC-UV peak areas (Fig 7), while more than 90% of the parent compound disappeared after the HRP incubation (Fig 6). Discordant percentage values exist between the disappearance of parent drug and the production of metabolites because other HRP oxidation products are not exhibited in Fig 7. More specifically, two unknown peaks in the LC-UV chromatogram, one eluting 3 min earlier than M_B1 and the other 0.5 min later than M_B1, were observed in the HRP incubate. Unfortunately, electrospray mass spectrometry did not reveal the chemical identities, not even the molecular masses for these two LC peaks. The unidentified LC-UV peaks were not detected in the incubations with human liver microsomes or CYP isoforms. Furthermore, the formation of the unidentified products could not occur in the absence of either HRP or H_2O_2.

DMD Fast Forward. Published on September 19, 2006 as DOI: 10.1124/dmd.106.012286
This article has not been copyedited and formatted. The final version may differ from this version.

DISCUSSION

Two chemical structural features were introduced upon N-alkylquinolinium metabolite formation: (i) a fixed charge that could exhibit notable characteristics in mass spectrometry; (ii) a polycyclic aromatic structure containing a heteroatom nitrogen, which may affect electronic spectra such as UV, etc. As summarized in Table 2, electrospray ionization produced dimer ions (two neutral molecules plus an ionizing H^+, Na^+ or K^+ ion) for compound **B** and its metabolites, except for M_B1. The exception of M_B1 can be easily rationalized, as Columbic repulsion would hinder two fixed-charged M_B1 ions adhering together in the gas phase. A different characteristic for the fixed charge of M_A3 was noted in the doubly charged ion $[M_A3+H]^{2+}$ at m/z (613+1)/2 = 307, with an intensity approximately 15% relative to the singly charged ion (M^+, m/z 613). The doubly charged ion was confirmed by LC-MS zoom scan around m/z 307 in an ion trap mass spectrometer, which revealed the expected half Dalton difference in m/z values between two adjacent isotopic ions. Doubly protonated ions did not occur for parent compound **A** and other common phase-I metabolites (such as *O*-dealkyl and phenyl-hydroxyl metabolites). Apparently, an M_A3 ion with the fixed charge is large enough to hold an additional proton at a basic site; reportedly, as did fixed-charged peptide derivatives consisting of 5 or 8 residues (Czeszak et al., 2004; Gu et al., 2000). Both compound **A** and **B** have multiple chromophores, therefore after the metabolic aromatization, the complete replacement of old UV absorption bands with new ones was not expected. Nonetheless, a new absorption band at λ_{max} 315 was recorded for M_B1 by a photodiode array UV detector. Likewise, a new band at λ_{max} 350 nm appeared for M_A3.

These λ_{max} values are in agreement with those previously reported for respective N-methylquinolinium or methoxy-N-methylquinolinium ions, e.g., 316 nm for N-methylquinolinium iodide in ethanol (Adams et al., 1955) or 342 nm for 6-methoxy-1-methylquinolinium bromide/iodide in water (Geddes et al., 2000). Fluorescence spectroscopy of the quinolinium metabolites was not investigated, although quinolinium is known to have fluorescent excitation/emission.

Ortiz de Montellano and De Voss have recently stated: "cytochrome P450 mechanisms continue to surprise and delight, although the field is growing to maturity and the completely unexpected is less frequently encountered" (Ortiz de Montellano and De Voss, 2005). Indeed, identifying unusual metabolites that are generated by plausible metabolic pathways are intriguing to scientists in the field. A postulated pathway for the formation of N-alkylquinolinium metabolites is proposed in Scheme 3. It has been reported that P450-mediated N-dealkylation of N,N-dialkylanilines occurs via single electron transfer (SET) from the heteroatom nitrogen, e.g., based on the low kinetic isotope effect of deuterium vs. hydrogen at the α-carbon on the N-dealkylation (Guengerich et al., 1996; Hollenberg et al., 1985; Miwa et al. 1983). Furthermore, the readily formation of the quinolinium metabolites of both **A** and **B** in HRP suggests that metabolic aromatization of the tetrahydroquinoline can be initiated via the SET mechanism, as the oxidation of aromatic amine by peroxidase is believed to undergo the amine free radical mechanism (Eling et al., 1991). It should also be noted that Shaffer et al. have previously discovered the HRP oxidation of N-methyl-1,2,3,4-tetrahydroquinoline to N-methylquinolinium during their investigation of the HRP

oxidation mechanism of N-cyclopropyl-N-methylaniline to an quinolinium ion (Scheme 2; Shaffer et al., 2001). Therefore, it is assumed that the P450-catalyzed aromatization of the alkyltetrahydroquinolines undergoes an initial SET step to generate a radical nitrogen cation (II; Scheme 3). The postulation of the pathway from structure IV to VI (Scheme 3) was originated from the radical mechanism for the P450-catalyzed oxidation of 4-alkyl-1,4-dihydropyridines derivatives bearing various substitutions (Augusto et al., 1982; Böcker and Guengerich 1986; Lee JS, 1988; Guengerich and Böcker, 1988). Augusto et al. reported the radical mechanism for the oxidation of the dihydropyridines on the basis of spin-trapping of the alkyl radical released from the 4-position (Augusto et al., 1982) and the mechanism was further supported by more evidence, e.g., no significant isotope effect for the 4-position hydrogen on the dehydrogenation (Guengerich and Böcker, 1988). An alternative mechanism, in which the oxidation of the 1,4-dihydropyridines can be mediated by trace iron cations outside the P450 active site and dependent on the presence of H_2O_2 produced by P450 uncoupling, has been suggested by one group (Kennedy and Mason, 1990). However, CYP3A4-catalyzed aromatization of the 1,4-dihydropyridines has been reported by another group with purified P450 enzymes in systems where lipid peroxidation was not possible and effects of metal chelators were not observed (Guengerich et al., 1991).

The dihydro intermediates III & IV, that would provide direct evidence for the postulated mechanism in Scheme 3, were not observed for either of the substrates. Likewise, Shaffer et al. did not detect similar dihydro intermediates in their HRP incubation of N-cyclopropyl-N-methylquinoline (Scheme 2; Shaffer et al., 2001). Their proposal of an

assumed 1-methyl-3,4-dihydroquinolinium intermediate was based on cyanide trapping of the iminium intermediate (Shaffer et al., 2001). On the contrary, dihydro intermediates in the formation of MPP^+ (Scheme 2; Castagnoli et al., 2002), N-methylisoquinolium (Scheme 2; Booth et al., 1989) and thienopyridinium (Dalvie and O'Connell, 2004) from their tetrahydro analogs have been clearly observed. Metabolites M_B2 and M_B8, appearing at m/z 309 in the LC-MS spectra, were once suspected to be dihydro intermediates from compound **B** (m/z 311). However, it was later discovered that the m/z 309 ion of M_B2 was an in-source fragment, formed by the loss of H_2O from the $[M+H]^+$ ion of the hydroxyl metabolite. Evidence included dimer ions of M_B2 (Table 2), as well as intact $[M-H]^-$ ions of M_B2 detected in negative ion electrospray LC-MS and the MS/MS spectrum of the $[M-H]^-$ ions (not shown). For M_B8 structural identification, the H/D exchange results (Table 2) permitted only two possibilities: (i) an iminium (with a fixed positive charge) that does not require an ionizing proton in electrospray — which however, would be contradictory to M_B8's retention time being slightly later than parent **B** in reversed-phase LC and would also not be supported by MS/MS (spectrum not shown); or (ii) a ring closed structure that eliminated the active hydrogen at the acyl aniline nitrogen of compound **B**. In short, M_B8 is clearly not a dihydroquinoline intermediate. The most likely structure of M_B8 (proposed in Fig 7) is the result of intramolecular trapping of the iminium intermediate of compound **B**, as strong evidence for iminium intermediates was obtained by cyanide trapping in liver microsomal incubations (Scheme 3).

In addition to the absence of dihydro intermediates, the absence of liver microsomal generated N-oxide metabolites for the N-alkyltetrahydroquinolines in the present study was another notable metabolism difference from the previously reported MPTP derivatives (Castagnoli et al., 2002; Bissel and Castagnoli, 2005) and other substructures somewhat similar to MPTP (Christensen et al., 1999; Dalvie and O'Connell, 2004). The active H/D exchange experiment provided evidence that none of the detected mono-oxidation metabolites of compound **B** were N-oxides. This difference in N-oxygenation is not surprising, since it has been reported that the rate of N-dealkylation *vs.* N-oxygenation is 940:1 in P450-catalyzed oxidation of N,N-dimethylaniline (Seto and Guengerich, 1993). On the other hand, the previously investigated substrates (cited above) have aliphatic tertiary amine nitrogen atoms which are prone to N-oxygenation.

Several relevant perplexing issues could not be addressed within the scope of this study. First, CYP3A4 is predominantly responsible for generating the quinolinium metabolites. It is unclear if this is merely another example of CYP3A4's great promiscuity (Smith, 2003) or a reflection of CYP3A4 being the principal participant in oxidation of tertiary amines (e.g., N-demethylation; Smith, 2003). Secondly, while the iminium intermediate from MPTP or N-methyl-tetrahydroisoquinoline is relatively stable (Scheme 2), the iminium intermediate III might be converted into IV (Scheme 3). Could IV be more easily converted to quinolinium than III? Could the rapid conversions (III $\rightarrow$ IV $\rightarrow$ quinolinium) explain the absence of dihydro intermediates? Thirdly, while MPTP and N-alkyltetrahydroisoquinoline have an aliphatic tertiary amine nitrogen (Scheme 2), the heteroatom in the N-alkyltetrahydroquinoline substructure is essentially a dialkylaniline

DMD Fast Forward. Published on September 19, 2006 as DOI: 10.1124/dmd.106.012286
This article has not been copyedited and formatted. The final version may differ from this version.

nitrogen. An N,N-dialkylaniline is relatively easier to form a radical cation than an aliphatic tertiary amine. Evidence can be readily gathered from the ionization energy (IE) of the analogs, measured in the gas phase for $M \rightarrow M^{+\bullet}$. For example, N,N-dimethylaniline has an IE of 7.12 ± 0.02 eV, while the IE is greater for N,N-dimethyl-N-benzylamine (7.69 ± 0.05 eV) which is very close to trimethylamine (7.85 ± 0.05 eV) (Lias, 2005). For comparison, toluene (absent of nitrogen) has an IE of 8.828 ± 0.001 eV (Lias, 2005). It is uncertain if the low IE of N,N-dialkylaniline implies that an N-alkyltetrahydroquinoline could be more prone to the SET oxidation mechanism (I to II; Scheme 3) than an N-alkyltetrahydroisoquinoline or MPTP like structure, an aliphatic tertiary amine with a benzylic or allylic methylene adjacent to the nitrogen. It would be our hope that the answers to these questions will be explored in the future.

ACKNOWLEDGEMENTS

Authors are grateful to the following Pfizer colleagues: Dr. Deepak Dalvie (La Jolla Laboratories), Dr. Benny M. Amore (Groton Laboratories) and Dr. Gwendolyn D. Fate (Ann Arbor Laboratories) for their insightful discussions and helpful suggestions. The authors would also like to thank Dr. Suzie A. Ferreira for requesting *in vitro* metabolite profiling of the renin discovery compounds including compound **A.** The authors are also indebted to Dr. G. D. Fate for manuscript revision suggestions.

REFERENCES

Adams JB, Cymerman-Craig J, Ralph C and Willis D. (1955) Iodination of N-methylquinolinium salts. *Aust J Chem* 8:392-402.

Augusto O, Beilan HS and Ortiz de Montellano PR (1982) The catalytic mechanism of cytochrome P450. *J Biol Chem* 257:11288-11295.

Barbieri G, Benassi R, Lazzeretti P, Schenetti L and Taddei F (1975) The ^{1}H NMR spectra of quinoline, quinoline N-oxide, the quinolinium ion and of their monomethyl derivatives. *Organic Magnetic Resonance* 7:451-454.

Bissel P and Castagnoli N Jr. (2005) Studies on the cytochrome P450 catalyzed oxidation of ^{13}C labeled 1-cyclopropyl-4-phenyl-1,2,3,6-tetrahydropyridine by ^{13}C NMR. *Bioorg Med Chem* 13:2975-2980.

Böcker RH and Guengerich FP (1986) Oxidation of 4-aryl and 4-alkyl-substituted 2,6-dimethyl-3,5-bis(alkoxycarbonyl)-1,4-dihydropyridines by human liver microsomes and immunochemical evidence for the involvement of a form of cytochrome P-450. *J Med Chem* 29:1596-1603.

Booth RG, Castagnoli N Jr. and Rollema H (1989) Intracerebral microdialysis neurotoxicity studies of quinoline and isoquinoline derivatives related to MPTP/MPP^{+}. *Neurosci Lett* 100:306-312.

Castagnoli N Jr., Castagnoli K, Magnin G, Kuttab S and Shang J (2002) Studies on the oxidation of 1,4-disubstituted-1,2,3,6-tetrahydropyridines. *Drug Metab Rev* 34:533-547.

Christensen EB, Andersen JB, Pedersen H, Jensen KG and Dalgaard L (1999) Metabolites of [^{14}C]-5-(2-ethyl-2H-tetrazol-5-yl)-1-methyl-1,2,3,6-tetrahydropyridine in mice, rats, dogs, and humans. *Drug Metab Dispos* 27:1341-1349.

Czeszak X, Morelle W, Ricart G, Tétaert D and Lemoine J (2004) Localization of the O-glycosylated sites in peptides by fixed-charge derivatization with a phosphonium group. *Anal Chem* 76: 4320-4324.

Dalvie DK, O'Connell TN (2004) Characterization of novel dihydrothienopyridinium and thienopyridinium metabolites of ticlopidine in vitro: Role of peroxidases, cytochromes P450 and monoamine oxidase. *Drug Metab Dispos* 32:49-57.

de Groot MJ, Vermeulen NPE, Kramer JD, van Acker FAA, Donne-Op den Kelder GM (1996) A three-dimensional protein model for human cytochrome P450 2D6 based on the crystal structures of P450 101, P450 102, and P450 108. *Chem Res Toxicol* 9:1079-91.

de Groot MJ, Bijloo GJ, van Acker FAA, Fonseca Guerra C, Snijders JG, Vermeulen NPE (1997) Extension of a predictive substrate model for human cytochrome P4502D6. Xenobiotica 27:357-368.

Di Monte DA, Royland JE, Irwin I and Langston JW (1996) Astrocytes as the site for bioactivation of neurotoxins. *Neurotoxicology* 17:697-704.

Eling TE, Curtis JF, Thompson DC, Van der Zee J and Mason RP (1991) Formation of aromatic amine free radical by prostaglandin hydroperoxidase and peroxyl radicals: analysis by ESR and stable end products, in *N-oxidation of Drugs: biochemistry, pharmacology, toxicology* (Hlavica P and Damani LA eds) pp 4-18, Chapman & Hall, New York.

Fisher NDL and Hollenberg NK (2005) Renin inhibition: what are the therapeutic opportunities? *J Am Soc Nephrol* 16:592-599.

Geddes CD, Apperson K and Birch DJS (2000) New fluorescent quinolinium dyes – application in nanometre particle sizing. *Dyes and Pigments* 44:69-74.

Gerlach M, Riederer P, Przuntek H and Youdim MBH (1991) MPTP mechanism of neurotoxicity and their implications for Parkinson's disease. *Eur J Pharmacol* 208:273-286.

Gu C, Tsaprailis G, Breci L and Wysocki VH (2000) Selective gas-phase cleavage at the peptide bond C-terminal to aspartic acid in fixed-charge derivatives of Asp-containing peptides. *Anal Chem* 72: 5804-5813.

Guengerich FP and Böcker RH (1988) Cytochrome P-450-catalyzed dehydrogenation of 1,4-dihydropyridines. *J Biol Chem* 263:8168-8175.

Guengerich FP, Brian WR, Iwasaki M, Sari MA, Bäärnhielm C and Berntsson P (1991) Oxidation of dihydropyridine calcium channel blockers and analogs by human liver cytochrome P-450 IIIA4 *J Med Chem* 34: 1838–1844.

Guengerich FP, Yun CH and Macdonald TL (1996) Evidence for a 1-electron oxidation mechanism in N-dealkylation of N, N-dialkylanilines by cytochrome P450 2B1. *J Biol Chem* 271:27321-27329.

Hollenberg PF, Niwa GT, Walsh JS, Dwyer LA, Rickert DE, and Kedderis GL (1985) Mechanism of N-demethylation reactions catalyzed by cytochrome P-450 and peroxidases. *Drug Metab Dispos* 13:272-275.

Holsworth DD, Powell NA, Downing DM, Cai C, Cody WL, Ryan JM, Ostroski R, Jalaie M, Bryant JW and Edmunds JJ (2005) Discovery of novel non-peptidic ketopiperazine-based renin inhibitors. *Bioorg & Med Chem.* 13:2657-2664.

Holsworth DD, Cai C, Cheng, X, Cody WL, Downing DM, Erasga N, Lee C, Powell NA, Edmunds JJ, Stier M, Jalaie M, Zhang E, McConnell P, Ryan MJ, Bryant J, Li T, Kasani A, Hall E, Subedi R, Rahim M and Maiti S. (2006) Ketopiperazine-based renin inhibitors: optimization of the "C" ring. *Bioorg Med Chem Lett.* 16:2500-2504.

Jurva U, Bissel P, Isin EM, Igarashi K, Kuttab S and Castagnoli N Jr. (2005) Model Electrochemical-Mass Spectrometric Studies of the Cytochrome P450-Catalyzed Oxidations of Cyclic Tertiary Allylamines. *J Am Chem Soc* 127:12368 - 12377

Kennedy CH, Mason RP (1990) A reexamination of the cytochrome P-450-catalyzed free radical production from a dihydropyridine. *J Biol Chem* 265:11425-11428.

Lee JS, Jacobsen NE and Ortiz de Montellano PR (1988) 4-Alkyl radical extrusion in the cytochrome P-450-catyalyzed oxidation of 4-alkyl-1,4-dihydropyridines. *Biochemistry* 27:7703-7710.

Lias SG (2005) Ionization Energy Evaluation, in NIST Chemistry WebBook, NIST Standard Reference Database Number 69, (Linstrom PJ and Mallard WG eds), National Institute of Standards and Technology (http://webbook.nist.gov).

Maret G, Testa B, Jenner P, El Taya N and Carrupt P-A (1990) The MPTP story: MAO activates tetrahydropyridine derivatives to toxins causing Parkinsonism. *Drug Metab Rev* 22:291-332.

Naoi M, Matsuura S, Parvez H, Takahashi T, Hirata Y, Minami M and Nagatsu T (1989) Oxidation of N-methyl-1,2,3,4-tetrahydroisoquinoline into the N-methyl-isoquinolinium Ion by monoamine oxidase. *J Neurochem* 52:653-655.

Miwa GT, Walsh JS, Kedderis GL, and Hollenberg PF (1983) The use of intramolecular isotope effects to distinguish between deprotonation and hydrogen atom abstraction mechanisms in cytochrome P-450- and peroxidase-catalyzed N-demethylation reactions *J Biol Chem* 258: 14445-14449.

Ortiz de Montellano PR and De Voss JJ (2005) Substrate oxidation by cytochrome P450 enzymes, in *Cytochrome P450: structure, mechanism, and biochemistry* (3rd edition, Ortiz de Montellano PR ed) pp 183-245, Kluwer Academic / Plenum Publishers, New York.

Seto Y and Guengerich FP (1993) Partitioning between N-dealkylation and N-oxygenation in the oxidation of N,N-dialkylarylamines catalyzed by cytochrome P450 2B1. *J Biol Chem* 268:9986-9997.

Shaffer CL, Morton MD and Hanzlik RP (2001) N-dealkylation of an N-cyclopropylamine by horseradish peroxidase: fate of the cyclopropyl group. *J Am Chem Soc* 123:8502-8508

Shaffer CL, Harriman S, Koen YM and Hanzlik RP (2002) Formation of cyclopropanone during cytochrome P450 catalyzed N-dealkylation of a cyclopropylamine. *J Am Chem Soc* 124:8268-8274.

Smith D. (2003), Cytochrome P450 and its place in drug discovery and development, in *Drug metabolizing enzymes: cytochrome P450 and other enzymes in drug discovery*

and development (Lee JS, Obach RS and Fisher MB eds) pp 155-177, Marcel Dekker Inc., New York.

Wood JM, Schnell CR, Cumin F, Menard J and Webb RL (2005) Aliskiren, a novel, orally effective renin inhibitor, lowers blood pressure in marmosets and spontaneously hypertensive rats. *J Hypertens* 23:417-426.

LEGENDS FOR SCHEMES

Scheme 1. Chemical structures of compounds **A** & **B**, and their respective quinolinium metabolites generated in human liver microsomes

Scheme 2. MPTP, N-methyltetrahydroisoquinoline vs. N-methyltetrahydroquinoline, and N-cyclopropyl-N-methylaniline

Scheme 3. Postulated mechanism of metabolic aromatization of an N-alkyl-1,2,3,4-tetrahydroquinoline

DMD Fast Forward. Published on September 19, 2006 as DOI: 10.1124/dmd.106.012286
This article has not been copyedited and formatted. The final version may differ from this version.

LEGENDS FOR FIGURES

Fig. 1. Human liver microsomal metabolite profiles of compound **A** recorded in **(a)** mass spectrometric total ion chromatogram (TIC) of m/z range 150-1000 Daltons; **(b)** UV chromatogram of absorption at 254 nm.

Fig. 2. LC-MS/MS product ion spectra acquired in a triple quadrupole instrument for **(a)** compound **A** and **(b)** its quinolinium metabolite M_A3. The ionizing proton for compound **A** is not shown in the chemical structure. Hydrogen transfers across a cleaved bond during the formation of some fragments are not shown in either of the chemical structures.

Fig. 3. One-dimensional ^{1}H NMR spectra showing aromatic proton regions of **(a)** the quinolinium metabolite *vs.* **(b)** its parent drug, compound **A**. Two-dimensional NMR TOCSY spectrum showing the quinolinium proton regions of metabolite M_A3 is provided in panel **c**. The ^{1}H peak at δ ~8.6 ppm and two ^{13}C satellite peaks are from formic acid or formate introduced in preparative LC.

Fig. 4. (a) The reconstructed ion chromatogram, consisting of the most abundant ions generated in electrospray ionization for compound **B** and its metabolites, acquired after a 60 min incubation of compound **B** in human liver microsomes; **(b)** The ion chromatogram, reconstructed in the same manner, acquired after the same microsomal incubation in the presence of 1 mM KCN.

Fig. 5. LC-MS/MS product ion spectra acquired in a triple quadrupole instrument for **(a)** compound **B, (b)** its quinolinium metabolite (M_B1), and **(c)** the cyano adduct of **B** formed in the cyanide trapping experiment. The cyano group is drawn at the

carbon adjacent to the nitrogen, as rationalized by the cyanide addition reaction to iminium. The ionizing proton for compound **B** or the cyano adduct is not shown in the chemical structures. Hydrogen transfers across a cleaved bond during the formation of some fragments are not shown in the chemical structures.

Fig. 6. Percent remaining of compound **B** after the incubation with a panel of cDNA-expressed human cytochrome P450 enzymes and horseradish peroxidase (HRP). The percentages were calculated from the LC-UV signal responses (at 250 nm plus at 315 nm) of compound **B** *vs*. the negative control incubations. The calculated values for 2A6, 2B6 and 2E1 were slightly greater than 100% but were displayed at 100%.

Fig. 7. Percent yields of the metabolites of compound **B,** produced by cDNA-expressed human cytochrome P450 enzymes and horseradish peroxidase (HRP). The percentages were estimated from the LC-UV peak area of a metabolite vs. the total area of compound **B** derived peaks, assisted by mass spectrometric signal responses if two metabolites co-eluted.

Table 1. Experimental conditions and parameters in LC-MS and preparative LC

Type of Experiment	Substrate	Column	Mobile Phase [a]	LC Instrument	Mass Spectrometer [b]
HLM Metabolite Profiling / Identification	**A**	Phenomenex® Synergi 4µ Hydro-RP 80A 150x2.00 mm	A: Water with 0.05% acetic acid; B: ACN with 0.05% acetic acid. 2%B for 2 min, linearly increased to 95%B over 25 min and held for 3 min. Flow rate: 0.30 mL/min.	Hewlett Packard 1100 Series (binary pump) with a double beam UV detector	LCQ Advantage ion trap for LC-MS profile shown; TSQ Quantum triple quadrupole with argon as collision gas for LC-MS/MS spectra shown
	B	Supelco Discovery® C18 5µm 150x2.1 mm	A: Water with 0.05% acetic acid; B: ACN with 0.05% acetic acid. Linear gradients of 5%B to 40%B over 10 min, to 55%B over next 15 min, to 95%B over another 10 min. Flow rate: 0.25 mL/min.	Finnigan Surveryor (quaternary pump) with a photodiode array (PDA) UV detector	LCQ Deca XP ion trap with helium as collision gas
Reaction Phenotyping with CYPs, MAOs or HRP	**A** & **B**	The same as above	The same as above	The same as above	LCQ Deca XP ion trap
Cyanide trapping of iminium intermediates.	**A** & **B**	The same as above	The same as above	The same as above	TSQ Quantum triple quadrupole
Active H/D exchange for HLM metabolites	**B**	The same as above	A: D_2O with 0.05% acetic acid-d_4; B: ACN with 0.05% acetic acid-d_4. The same gradients as above were applied.	The same as above	LCQ Deca XP ion trap
Metabolite Isolation Using Preparative LC	**A** [c]	Phenomenex® Luna 5µ C18(2) 150x21.20 mm	A: Water with 0.05% acetic acid; B: ACN. 2%B for 2 min, linearly increased to 45%B over 85 min, then immediately raised to 100%B and held for 3 min. Flow rate: 20 mL/min.	Agilent 1100 Series preparative system	N/A

[a] Columns were equilibrated for 15 min before next injection.
[b] Operated in positive ion electrospray.
[c] Unchanged compound **A** and its quinolinium metabolite M_A3 eluted at approximately 61 and 36.5 min; respectively, with the preparative LC method.

Table 2. Electrospray ionization generated ions (monomer and/or non-covalent dimer) of compound B and its metabolites before and after active H/D exchange in LC-MS using deuterated solvent.

	m/z range of monomer			m/z range of dimer			Explanation	
	M^+	$[M + H/D]^+$	In source fragment by loss of a water molecule from $[M + H/D]^+$	$[2\times M + H/D]^+$	$[2\times M + Na]^+$	$[2\times M + K]^+$	MW	# of Exchangeable H
Cmpd **B**		311 → 313			643 → 645	n.d. → 661*	310	1
M_B1	307 → 308						307**	1 (no need for an ionizing H)
M_B2		n.d.	309 → 311		675 → 679	691 → 695	326	2
M_B3		325 → 327		649 → 652	671 → n.d.*		324	1
M_B4		283 → 286			587 → 591(w)*	n.d. → 607*	282	2
M_B5		325 → 327			671 → n.d.*		324	1
M_B6		327 → 330			675 → n.d.*	n.d. → 695*	326	2
M_B7		325 (w) → 327 (w)	307 → 308&307		671 → n.d.*		324	1
M_B8		309 → 310		617 → 618	639 → 639		308	0

n.d. = not detected

(w) = (weak)

* The different abundances of sodium or potassium adduct ions before and after H/D exchange could be caused by different trace levels of sodium vs. potassium (e.g., leaked out of glass) in different LC mobile phases.

** A positive ion with a fixed charge.

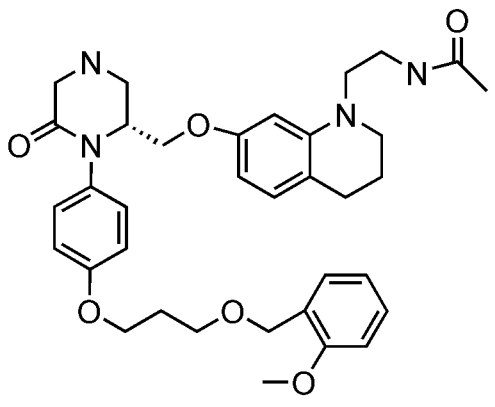

A

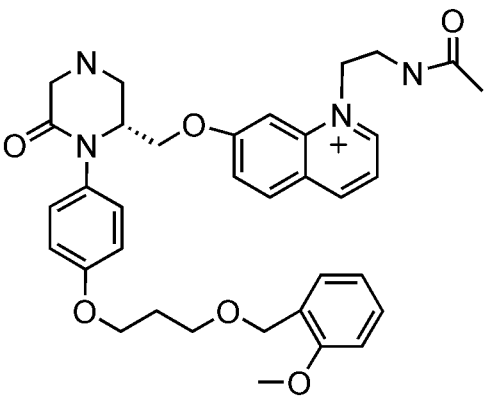

quinolinium metabolite

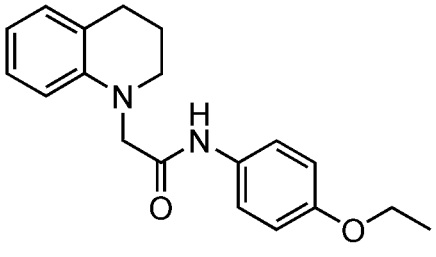

B

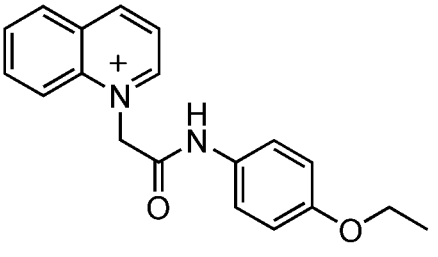

quinolinium metabolite

Scheme 1

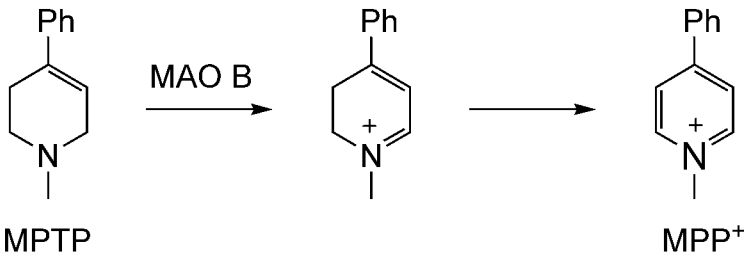

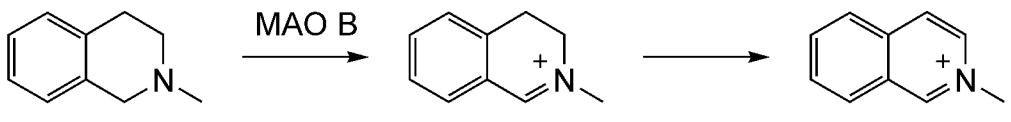

N-methyl-tetrahydroisoquinoline

N-methyl-isoquinolinium

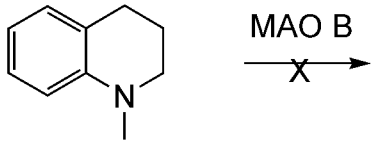

N-methyl-tetrahydroquinoline

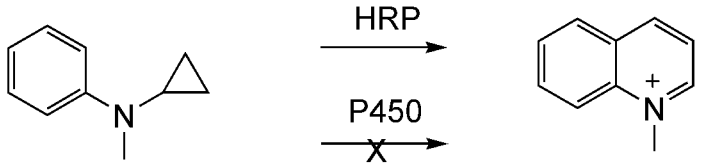

N-cyclopropyl-N-methylaniline

N-methyl-quinolinium

Scheme 2

DMD Fast Forward. Published on September 19, 2006 as DOI: 10.1124/dmd.106.012286
This article has not been copyedited and formatted. The final version may differ from this version.

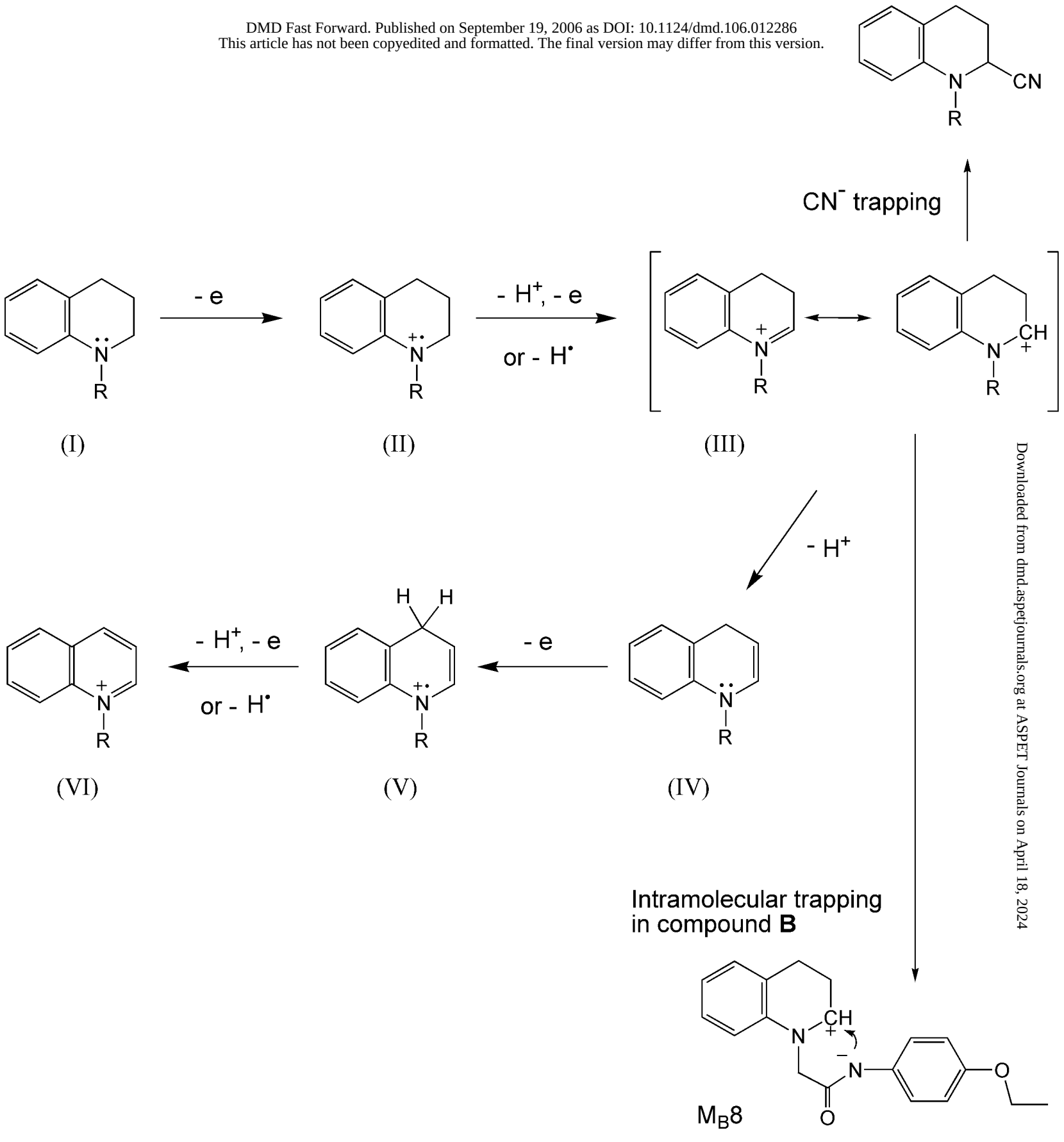

Scheme 3

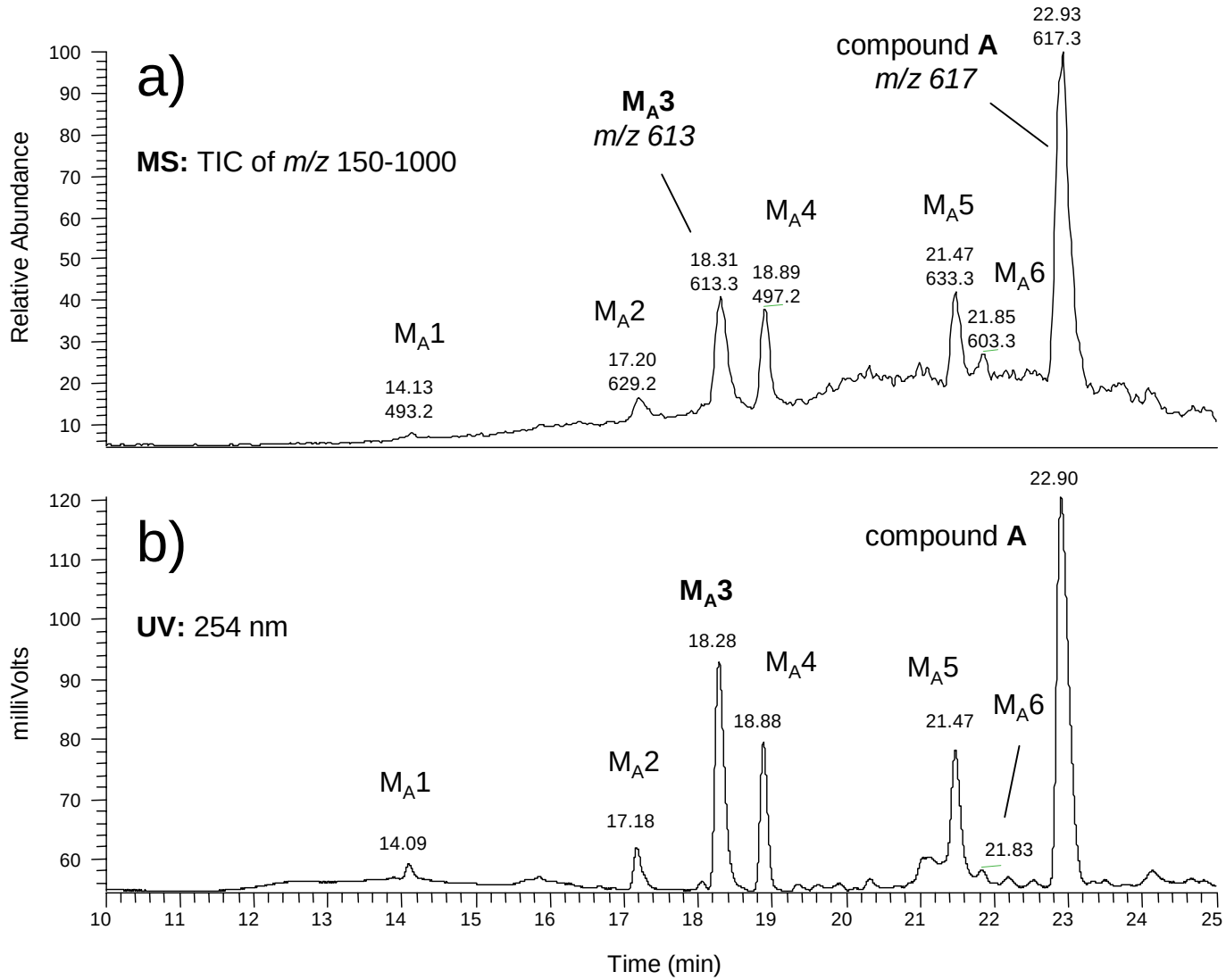

Fig 1

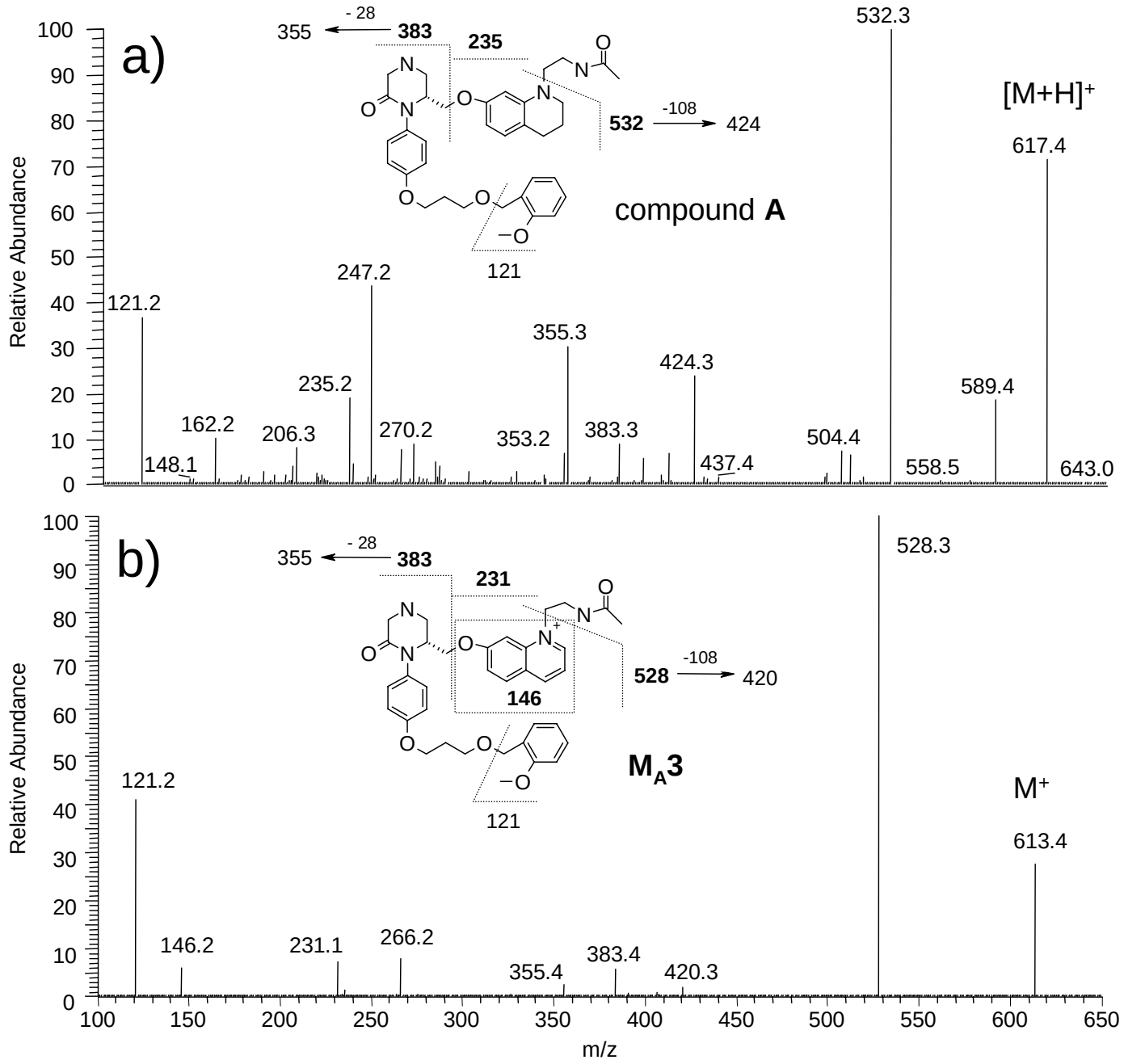

Fig 2

DMD Fast Forward. Published on September 19, 2006 as DOI: 10.1124/dmd.106.012286
This article has not been copyedited and formatted. The final version may differ from this version.

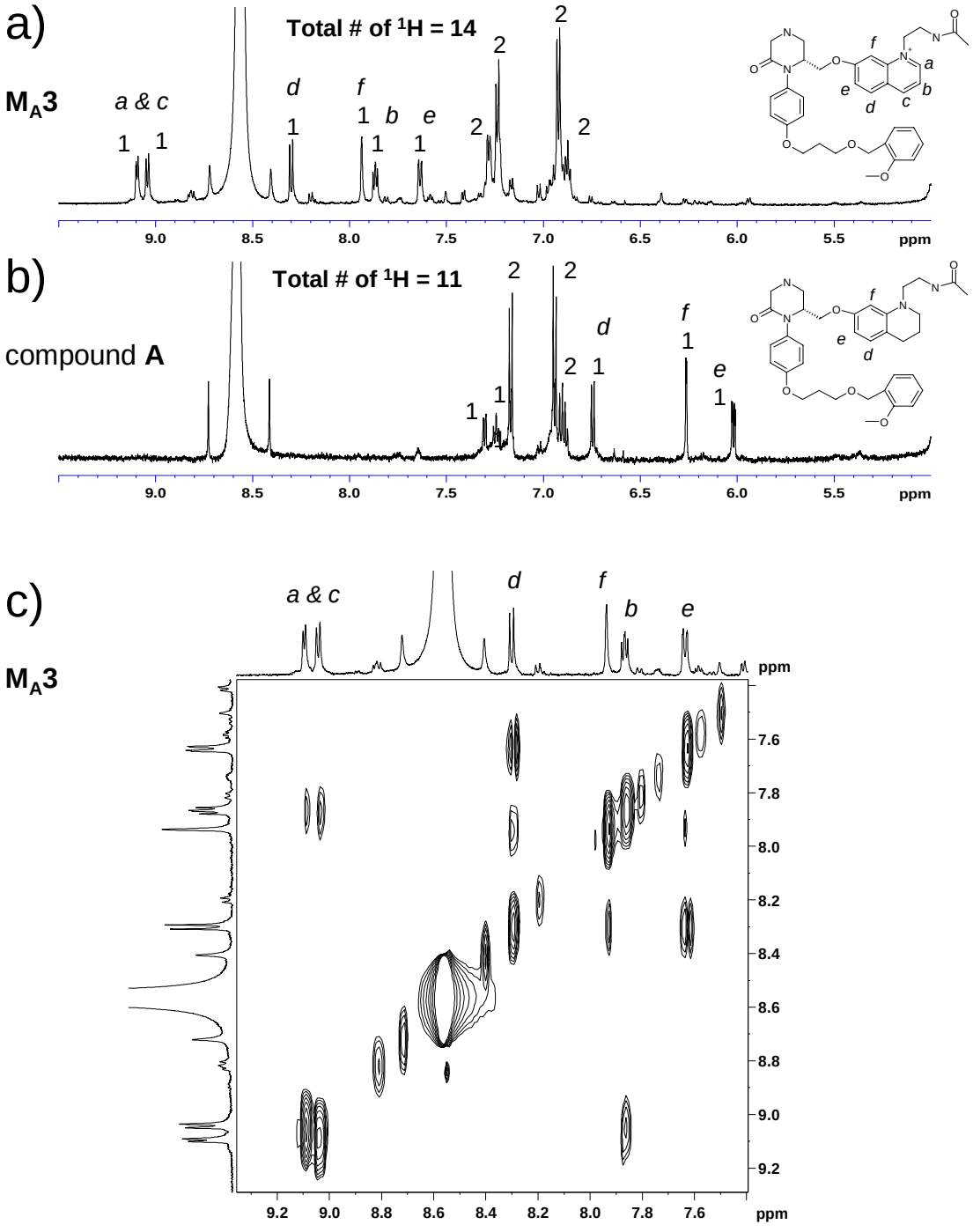

Fig 3

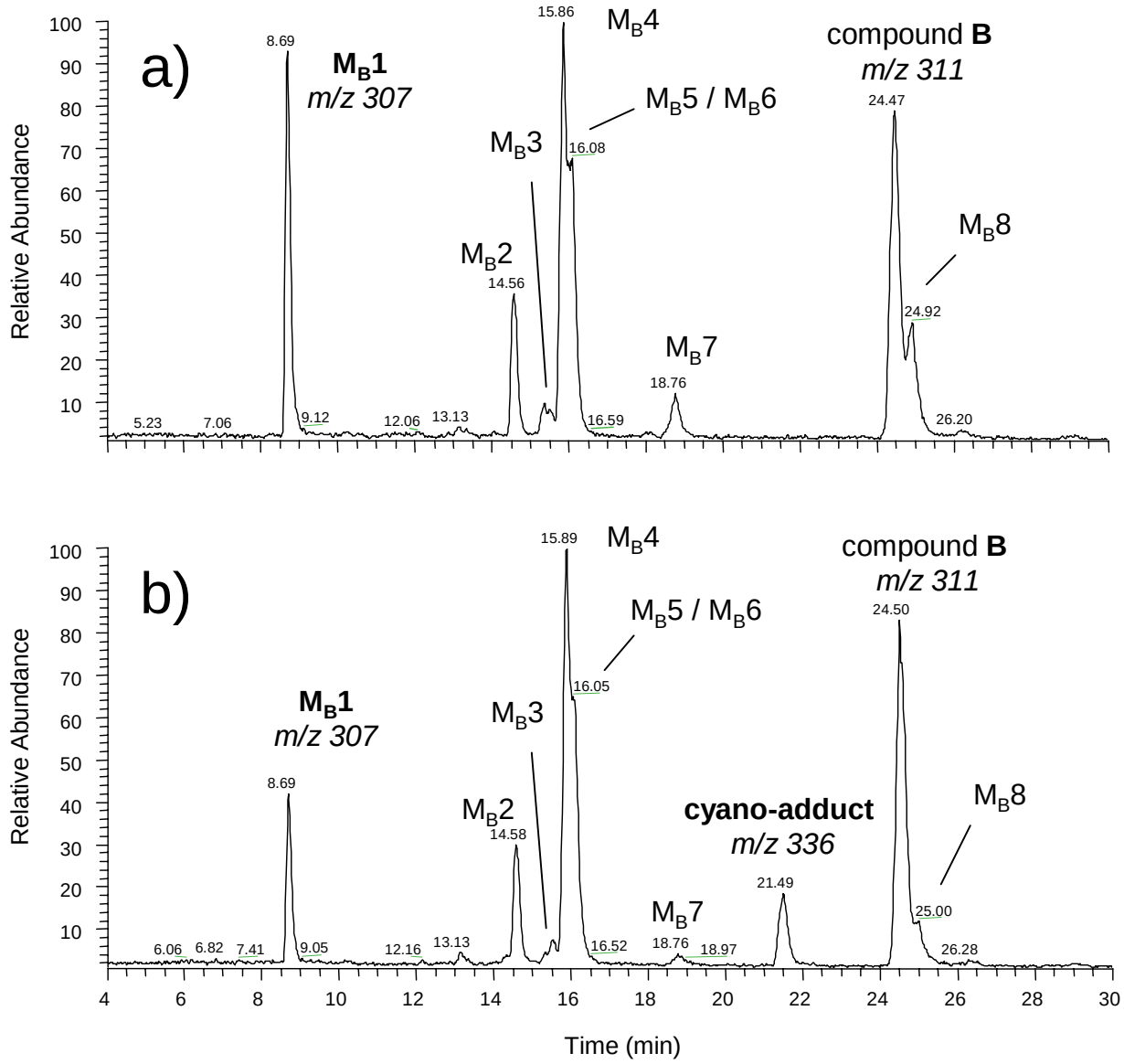

Fig 4

DMD Fast Forward. Published on September 19, 2006 as DOI: 10.1124/dmd.106.012286
This article has not been copyedited and formatted. The final version may differ from this version.

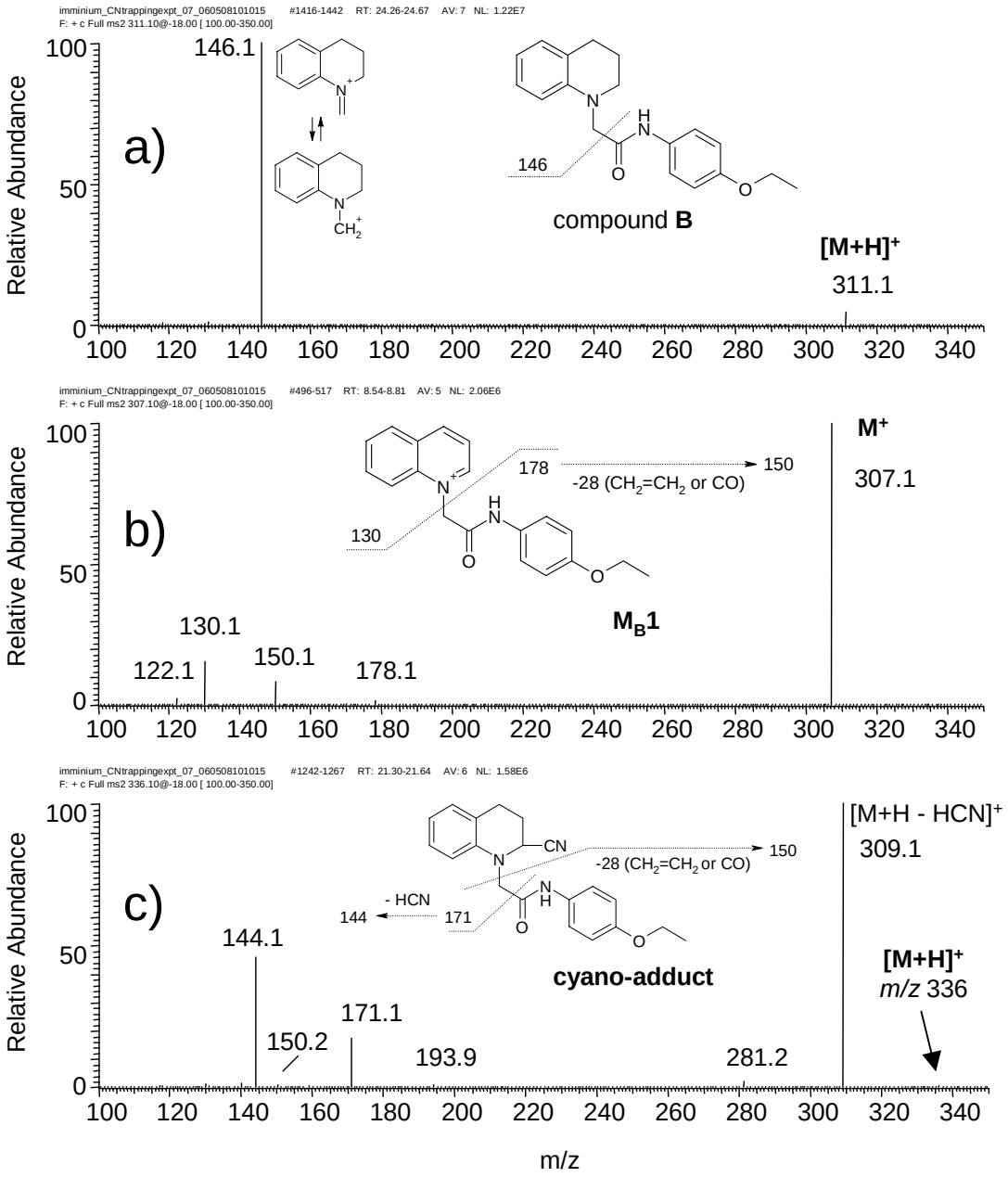

Fig 5

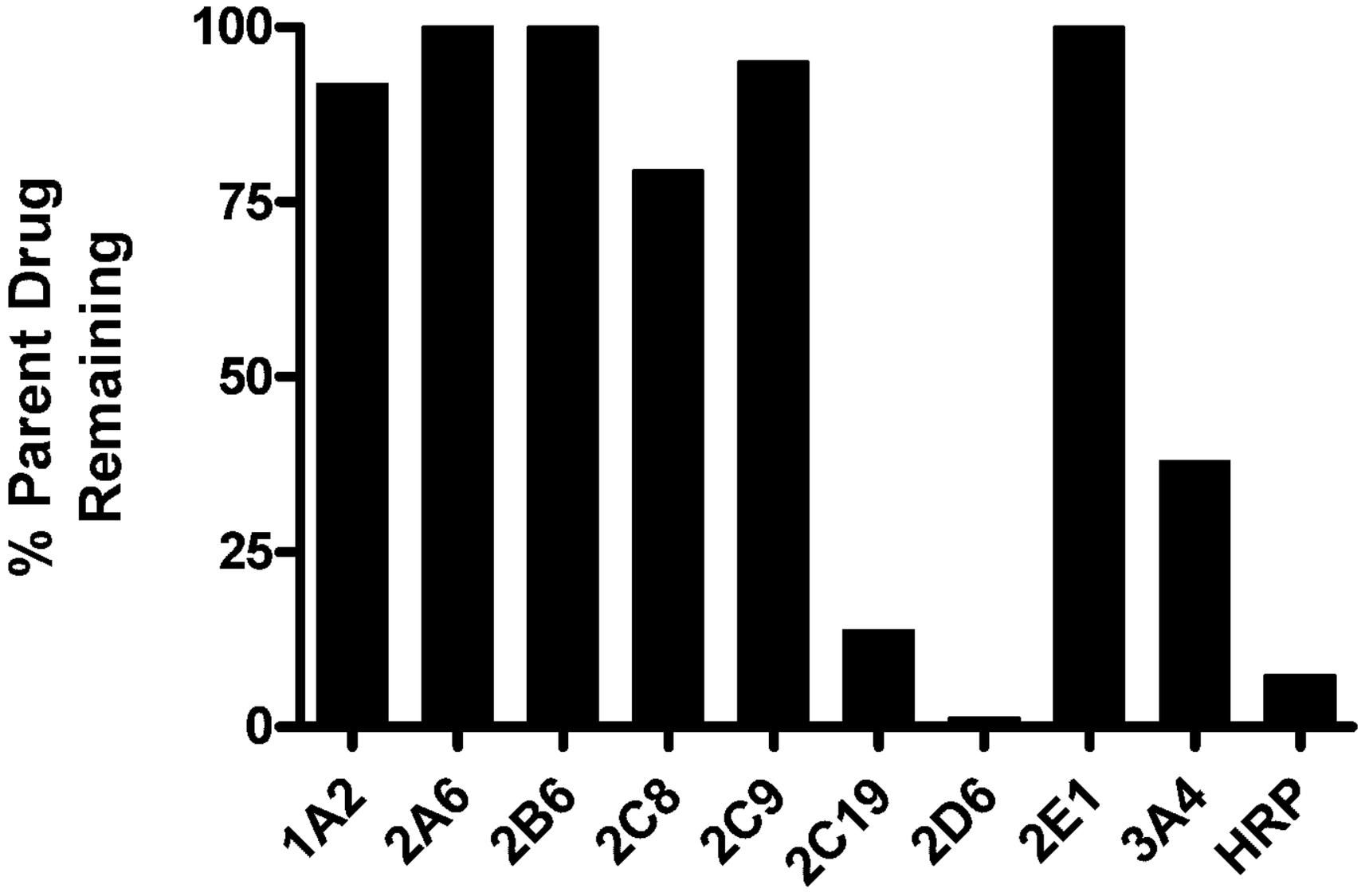
% Parent Drug Remaining
100
75
50
25
0
1A2
2A6
2B6
2C8
2C9
2C19
2D6
2E1
3A4
HRP

Fig 6

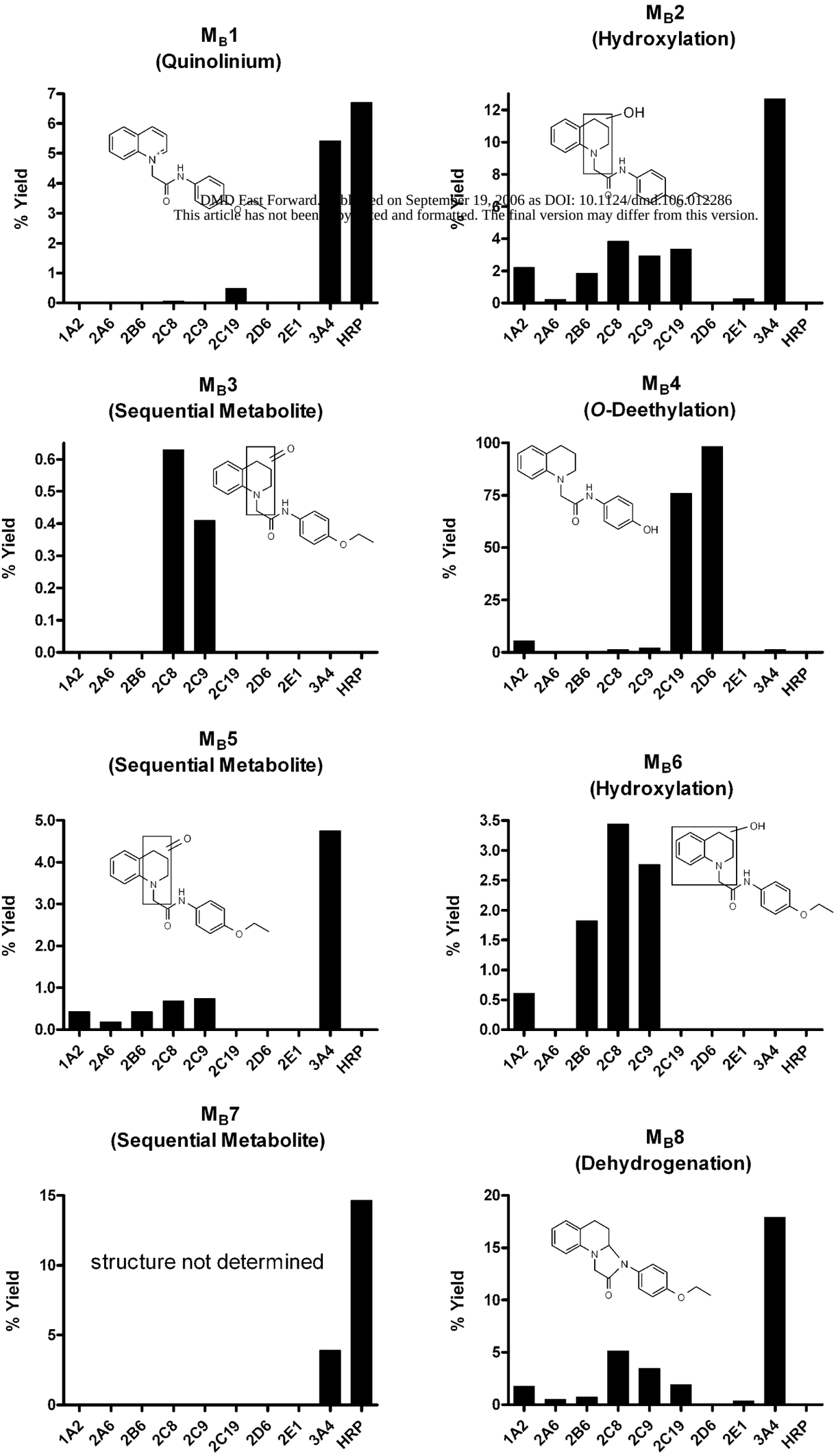

Fig 7